Imaging, Spectroscopic, Mechanical and Biocompatibility Studies of Electrospun Tecoflex(®) EG 80A Nanofibers and Composites Thereof Containing Multiwalled Carbon Nanotubes

ARTICLE *in* APPLIED SURFACE SCIENCE · DECEMBER 2014

Impact Factor: 2.71 · DOI: 10.1016/j.apsusc.2014.09.198

Applied Surface Science 321 (2014) 205–213

Contents lists available at ScienceDirect

Applied Surface Science

journal homepage: www.elsevier.com/locate/apsusc

Imaging, spectroscopic, mechanical and biocompatibility studies of electrospun Tecoflex® EG 80A nanofibers and composites thereof containing multiwalled carbon nanotubes

Javier Macossay[a,*], Faheem A. Sheikh[a,b], Travis Cantu[a], Thomas M. Eubanks[a], M. Esther Salinas[a], Chakavak S. Farhangi[a], Hassan Ahmad[a], M. Shamshi Hassan[c], Myung-seob Khil[c], Shivani K. Maffi[d,e], Hern Kim[f], Gary l. Bowlin[g]

[a] Department of Chemistry, University of Texas-Pan American, Edinburg TX 78539, USA
[b] Nano-Bio Regenerative Medical Institute, College of Medicine, Hallym University, Chuncheon 200-702, South Korea
[c] Department of Organic Materials and Fiber Engineering, Chonbuk National University, Jeonju 561-756, South Korea
[d] Regional Academic Health Center-Edinburg (E-RAHC), Medical Research Division, 1214 W. Schunior St, Edinburg TX 78541USA
[e] Department of Molecular Medicine, University of Texas Health Science Center, 15355 Lambda Dr. San Antonio TX 78245USA
[f] Energy and Environment Fusion Technology Center, Department of Energy and Biotechnology, Myongji University, Yongin Kyonggi-do 449-728, Republic of Korea
[g] Department of Biomedical Engineering, The University of Memphis, Memphis TN 38152, USA

ARTICLE INFO

Article history:
Received 23 July 2014
Received in revised form
29 September 2014
Accepted 30 September 2014
Available online 7 October 2014

Keywords:
Nanofibers
Electrospinning
Nanotechnology
Tissue engineering
Fibroblasts
Multiwalled carbon nanotubes

ABSTRACT

The present study discusses the design, development, and characterization of electrospun Tecoflex® EG 80A class of polyurethane nanofibers and the incorporation of multiwalled carbon nanotubes (MWCNTs) to these materials. Scanning electron microscopy results confirmed the presence of polymer nanofibers, which showed a decrease in fiber diameter at 0.5% wt. and 1% wt. MWCNTs loadings, while transmission electron microscopy showed evidence of the MWCNTs embedded within the polymer matrix. The Fourier transform infrared spectroscopy and Raman spectroscopy were used to elucidate the polymer-MWCNTs intermolecular interactions, indicating that the C–N and N–H bonds in polyurethanes are responsible for the interactions with MWCNTs. Furthermore, tensile testing indicated an increase in the Young's modulus of the nanofibers as the MWCNTs concentration was increased. Finally, NIH 3T3 fibroblasts were seeded on the obtained nanofibers, demonstrating cell biocompatibility and proliferation. Therefore, the results indicate the successful formation of polyurethane nanofibers with enhanced mechanical properties, and demonstrate their biocompatibility, suggesting their potential application in biomedical areas.

1. Introduction

A simple experimental setup to produce polymeric fibers by using high voltages and the process was named as electrospinning attracted much attention in the late 1990s, when a variety of fibers were electrospun and their potential applications were foreseen [1]. A basic electrospinning process consists of a polymer solution supplied through a nozzle while being connected to a high voltage power supply, which causes the formation of a droplet cone, known as the Taylor cone, at the nozzle tip. An electrically charged polymer jet forms at the tip of this cone and is ejected initially in a straight path, but it undergoes an electrical bending instability as it travels to a grounded collector. As a result of these events, the solvent in the polymer solution evaporates to afford solidified micro- and nanofibers on the grounded collector [1,2]. Potential applications of these fibers are vast, including filtration devices, sensors, composites, and tissue engineering applications [3–8].

Polyurethane (PU) elastomers are a broad family of segmented block copolymers consisting of hard crystalline segments dispersed between flexible amorphous segments. The hard segments are made of aliphatic or aromatic diisocyanates, which promote intermolecular hydrogen bonding and result in the glassy or crystalline phase that imparts toughness to the material. In contrast, the soft segments usually consist of polyethers, polybutadienes or polyesters, which are responsible for the formation of elastomeric domains that provide flexibility and elastic recovery to the polymer. The chemical, mechanical, and biocompatibility properties of PUs prompted the study of these polymers for biomedical

* Corresponding author. Tel.: +956 665 3377; fax: +956 665 5006.
E-mail address: jmacossay@utpa.edu (J. Macossay).

http://dx.doi.org/10.1016/j.apsusc.2014.09.198
0169-4332/

applications since the 1960s [9,10], resulting in current commercial products that include cardiovascular devices, breast implant linings, catheters, and others [11], while other polyurethanes could potentially be used as biosensors, protective clothing, and tissue engineering applications [11–14].

Single walled and multiwalled carbon nanotubes (SWCNTs and MWCNTs, respectively) are carbonaceous materials with strong conjugated C–C sp^2 bonds that result in a hexagonal network capable of distortions for relaxing stress [15–17]. These carbon allotropes present a Young's modulus of approximately 1 TPa and tensile strength from 13 to 53 GPa for SWCNTs, and a Young's modulus of 0.9 TPa and tensile strength up to 150 GPa for MWCNTs [16–19]. The result of these chemical and physical properties is high strength, flexibility, and stiffness, so these materials are attractive as polymer additives for enhancing the mechanical properties of polymer matrices.

Tissue engineering was defined as the confluence of clinical medicine, engineering, and science in a 2003 by National Science Foundation (NSF), report [20]. Therefore, to promote the development of this promising multidisciplinary field, it is required to develop new polymers and assess the available ones for scaffolds, according to their nature. As aforementioned, the nanofibers obtained via electrospinning approach had also influenced the tissue regeneration techniques. For instance, scaffolds made for improvement in ocular surface bioengineering using poly-ε-caprolactone nanofibers [21], co-electrospinning of poly(l-lactide), and polydimethylsiloxane to regulate smooth muscle growth [22], orientation of smooth muscle cells towards aligned polyurethane/collagen nanofibers [23] various uses of carbon fibers in improvement of mechanical properties and retaining biocompatibility had been well documented [24] and 3 D porous nanofiber membranes using poly-ε-caprolactone-MWCNTs for scaffold application [25]. However, all these reports suggest the initial potential applications, which are not well directed towards the polymer interaction with nano-size filler, mechanical properties, and biocompatibility assays, for use of nanofibers in creating artificial tendon and ligaments. Hence, this paper reports the successful electrospinning of a medical grade segmented polyurethane (Tecoflex® EG-80A) to obtain polymer nanofibers. Furthermore, incorporation of MWCNTs to the electrospun nanofibers with the objective of enhancing their mechanical properties was achieved, followed by extensive characterization through imaging (SEM and TEM), spectroscopic (FTIR and Raman), and tensile testing. In addition, assessment of the nanofibers biocompatibility was evaluated using NIH 3T3 fibroblasts, indicating that the materials prepared are potentially suitable in tissue engineering applications.

2. Materials and methods

Tecoflex® EG-80A was kindly supplied by Lubrizol Advanced Materials. Tetrahydrofuran (THF, 99+%) and N,N-dimethylformamide (DMF, 99.8%) were purchased from Sigma-Aldrich and used without further purification. MWCNTs (Baytubes® C 150 HP outer diameter of ~13 nm, inner diameter of ~4 nm and length of >1 μm) were kindly supplied by Bayer Materials. Mouse embryonic NIH 3T3 fibroblasts were purchased from ATCC (Manassas, VA). Dulbecco's Modified Eagle Medium (DMEM) supplemented with 10% newborn calf serum (NBCS), 7.5% sodium bicarbonate, and 1% antibiotic-antimycotic 100× (10,000 units/mL of penicillin, 10,000 μg/mL of streptomycin, and 25 μg/mL of amphotericin B) were obtained from Invitrogen. 3-[4,5-dimethylthiazol-2-yl]-2,5-diphenyl tetrazolium bromide (MTT reagent) and Dimethyl sulfoxide (DMSO, ≥99.9%) were acquired from Sigma-Aldrich, 0.4% Trypan blue and 0.25% Trypsin-EDTA for cell harvest from Invitrogen. Glycine was purchased from BioRad Laboratories to form glycine buffer, which was prepared by taking 0.1 M glycine containing 0.1 M NaCl, followed by equilibration with 0.1 N NaOH to pH = 10.5. Treated tissue culture flasks and microplates for cell growth and seeding were purchased from Fisher Scientific.

2.1. Preparation of polymeric solutions and polymer-MWCNTs dispersions

A 10% wt. Tecoflex® EG-80A solution was prepared by dissolving the polymer in a mixture of THF: DMF (1:1). The polymer-MWCNTs dispersions were prepared by placing the MWCNTs in DMF at 0.1, 0.5, and 1% wt. with respect to the polymer, and sonicated using a 500 watt ultrasonic processor (Sonics Vibra-cell model VCX 500) operating at 20 kHz with amplitude of 20% for all the samples using a standard probe. The dispersions were sonicated for 1 h in an ice bath to avoid excessive heat generated during the process, affording a black-ink like appearance that did not show precipitates for two months. These dispersions were prepared and immediately added to a previously dissolved Tecoflex® EG-80A solution in THF, resulting in a 10% wt. polymer with 0.1, 0.5, and 1.0% wt. MWCNTs.

2.2. Electrospinning process

The polymer solutions and the polymer-MWCNTs dispersions were placed in a 10 mL glass syringe with a 22 needle gauge (0.7 mm OD × 0.4 mm ID) at a flow rate of 0.02 mL/min, which was controlled using a KDS 210 pump (KD Scientific Holliston, Inc., MA). High power voltage supplies (ES30P-5 W and ES30N-5 W for positive and negative voltages, respectively) were purchased from Gamma High Voltage Research (Ormond Beach, FL). The positive electrode was used to apply a voltage of +15 kV to the needle tip through an alligator clip, while the negative electrode was set to an applied voltage of −15 kV to the collector. The polymer solution and the polymer-MWCNTs dispersions were electrospun at a 15 cm distance between the needle tip and the rounded rotating collector. The electrospun nanofibers were dried under vacuum for 24 h in the presence of P_2O_5 to remove any possible traces of residual moisture and solvents.

2.3. Cell seeding

NIH 3T3 fibroblasts from ATCC were obtained in a frozen ampoule and allowed to propagate in a 25 cm^2 culture treated flask. After reaching 70–80% confluence, the cells were inoculated and sub-cultured. The fibroblasts were maintained with DMEM supplemented with 10% newborn calf serum (NBCS), 7.5% sodium bicarbonate, and 1% antibiotic-antimycotic 100× (10,000 units/mL of penicillin, 10,000 μg/mL of streptomycin, and 25 μg/mL of amphotericin B). The flask containing the cells was kept in a humidified incubator with 5% CO_2 environment at 37 °C and the culture media was renewed twice a week. After 80% confluence, the cells were harvested with 0.25% Trypsin-EDTA, resuspended with DMEM and used to perform compatibilty assays. Cell seeding was performed by using a 25,000 cells/mL solution, using a Countess® automated cell counter to ensure cell density. A total of 160 μL aliquot of the 25,000 cells/mL solution was added into 96-well microplates and allowed to proliferate for 24 h in 5% CO_2 environment at 37 °C. Meanwhile, nanofibers were cut with 6 mm skin biopsy punches (Acuderm, Inc.) and sterilized for 12 h under UV irradiation [26]. After the 24 h incubation period, the existing media was removed and 80 μL of fresh DMEM supplemented as described before was added to the wells, followed by the placement of the already sterilized polymers inside the individual wells; these

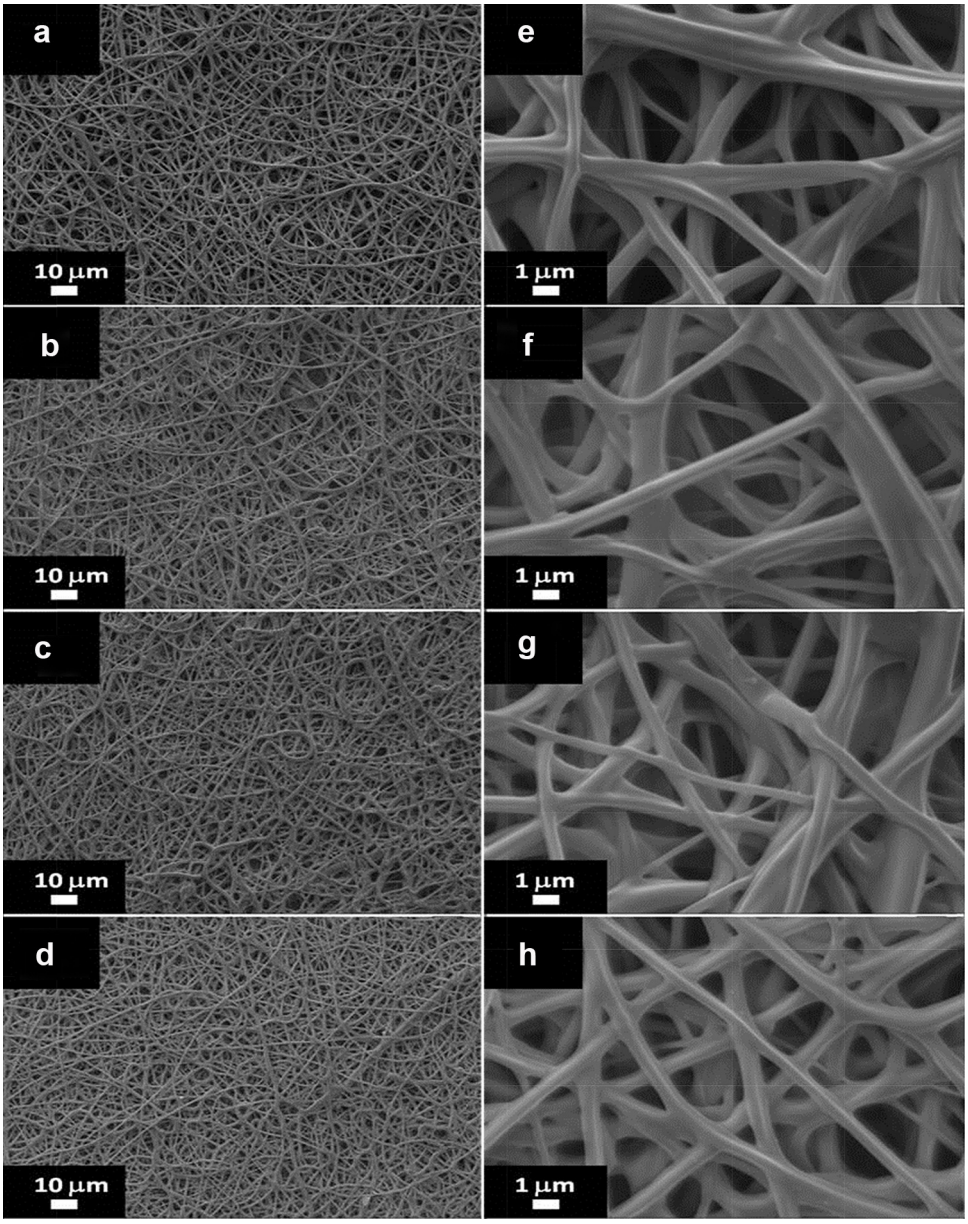

Fig. 1. SEM images for nanofibers containing different amounts of MWCNTs (a) 0% wt., (b) 0.1% wt., (c) 0.5% wt., and (d) 1% wt. at 1.5 K magnification. Corresponding figures containing (e) 0% wt., (f) 0.1% wt., (g) 0.5% wt., and (h) 1% wt. at 15 K magnification.

assays were performed in triplicate. A total of 80 μL of DMEM supplemented as described before were added to complete a 160 μL final volume of fresh media, both for experimental and blank wells. Finally, the cell culture microplates containing NIH 3T3 fibroblasts and nanofibers were incubated and allowed to proliferate for 1, 3, and 7 days. Exhausted media was replenished at the 3 day mark.

2.4. Nanofibers biocompatibility

After the designated culture periods, the media was completely removed from the wells containing pristine nanofibers, PU-MWCNTs, and blanks, and replaced with 160 μL of DMEM supplemented as described before without phenol red. A total of 5 mg/mL solution of MTT reagent in phosphate buffer saline (PBS) was prepared, from which a 40 μL aliquot was added to the wells in the microplates and incubated for 4 h. During the incubation period, metabolically active cells' enzymes reacted with the MTT solution to produce a purple coloration. Subsequently, the microplates were centrifuged at 1097.6 g for 10 min, and the existing DMEM without phenol red and MTT solution were removed and replaced with 160 μL of DMSO and 20 μL of glycine buffer. The microplates were placed on a shaker for 5 min to allow the solutions to mix, and all nanofibers were carefully removed from each well to prevent interference. Spectrophotometric readings were obtained using a microplate reader at 595 nm (Bio-rad model 680).

2.5. Statistical analysis

Statistical analysis was performed using SPSS version 19. For fiber diameter, breaking stress, breaking strain, Young's modulus, maximum peak load, and energy at maximum load analysis, a one-way ANOVA with Fisher's LSD post-hoc test was used to evaluate the differences between groups. For NIH 3T3 fibroblasts proliferation using the MTT assay, a two-way ANOVA with Fisher's LSD *post*

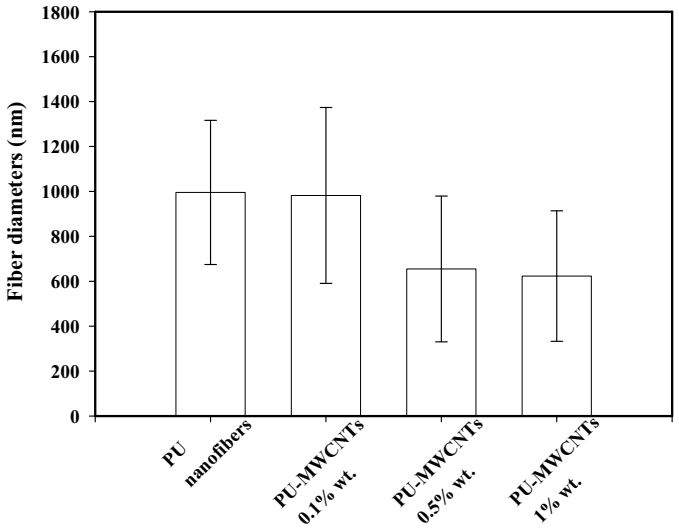

Fig. 2. Fiber diameter for PU nanofibers and PU-MWCNTs.

priori test was used. Results are reported as mean ± standard deviation and a p value ≤ 0.05 was considered statistically significant.

2.6. Scanning electron microscopy

Scanning electron microscopy (SEM) using an EVO® LS10 (Carl Zeiss Microscopy) was utilized to investigate the electrospun nanofibers morphology (10 individual diameters were measured per sample to calculate the average fiber diameter). The samples were coated with a thin layer of silver-palladium for 180 s at 45 mA with a Desk II Denton Vacuum Cold Sputter. After coating, the micrographs were taken at an accelerating voltage of 10.75 kV.

2.7. Transmission electron microscopy

Transmission electron microscopy (TEM) of MWCNTs and nanofibers containing MWCNTS was performed using a JEOL JEM 2010 operating at 200 kV (JEOL Ltd.). The samples for TEM of MWCNTs were prepared by sonicating (as described in Section 2.2.1) a 1 mg/mL aqueous dispersion of MWCNTs, followed by placing a drop of the solution on a TEM copper grid, which was allowed to dry overnight under vacuum. To prepare the samples of PU and PU/MWCNTs, embedded with or without the electrospun nanofibers was investigated by placing a TEM grid close to the tip of the syringe needle for a few seconds during the electrospinning process, followed by vacuum drying and TEM analysis.

2.8. Fourier transform infrared spectroscopy and Raman spectroscopy

The polymer structure and its interactions with the MWCNTs were investigated through Fourier transform infrared spectroscopy (FTIR). The spectra were recorded by grinding fiber samples with KBr to form pellets, which were analyzed using a Bruker spectrophotometer (IFS 55) from 4000 to 700 cm^{-1} with a 4 cm^{-1} resolution and 32 scans. Raman spectra for the pure MWCNTs and the nanofibers were obtained on a Bruker Optics Raman Spectrometer (B×51) at 785 nm laser excitation. The laser power density was kept as 10 mW with 50 integrations, 2 co-additions and 25 × 100 nm of aperture. Spectra were collected at various locations using a microscope with 50× magnification on each sample.

2.9. Tensile testing

The mechanical behavior of the nanofiber mats was investigated using an INSTRON® tensile tester 5943 with a 25 N maximum load cell under a crosshead speed of 10 mm/min. The samples utilized for mechanical characterization were cut from nonwoven mats in

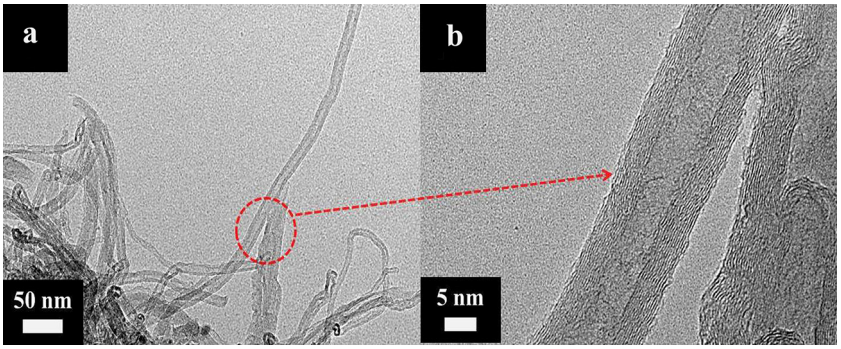

Fig. 3. TEM images for pristine MWCNTs (a) agglomerated in bundles, and (b) magnification of the indicated area.

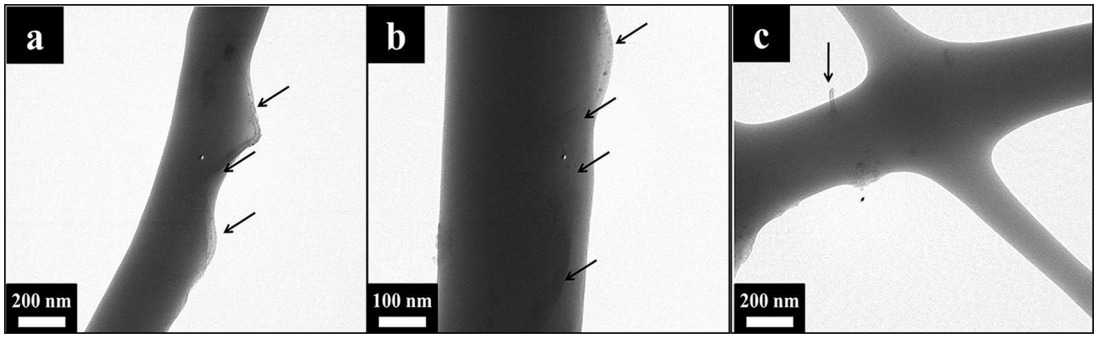

Fig. 4. TEM micrographs of (a) and (b) MWCNTs oriented along the PU nanofiber; (c) MWCNT protruding from the PU nanofiber.

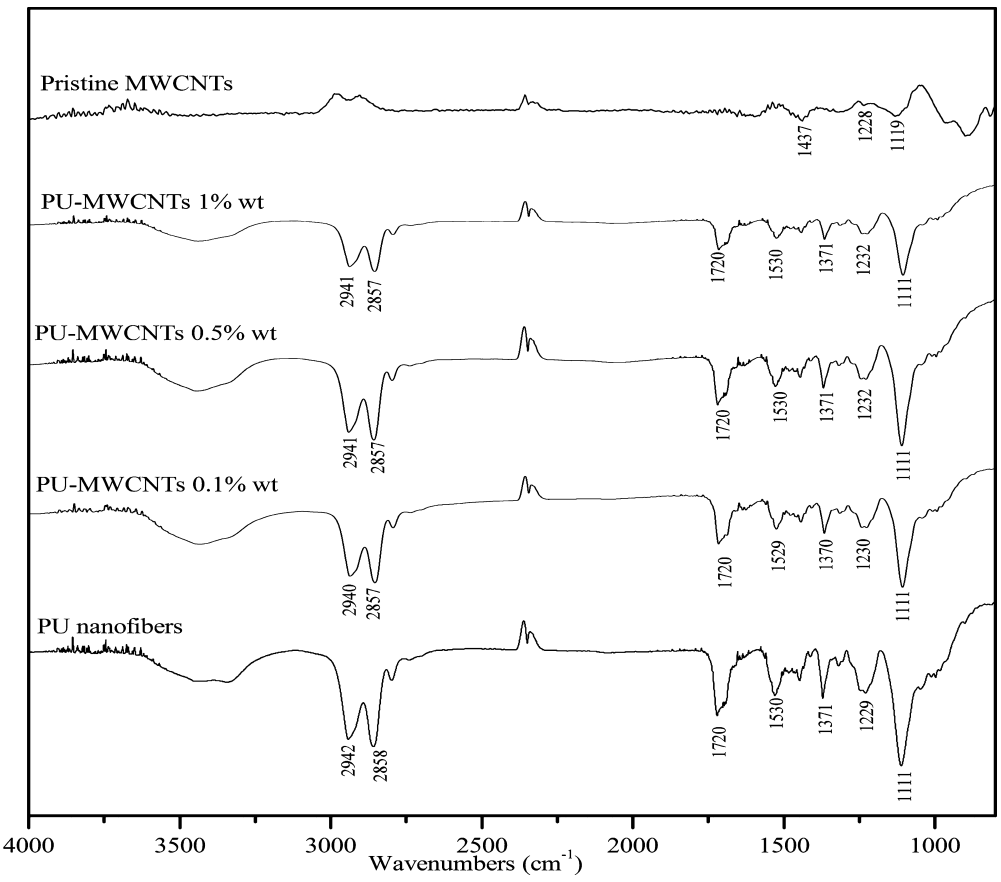

Fig. 5. FTIR spectra of MWCNTs, polymer nanofiber and corresponding nanofibers containing MWCNTs.

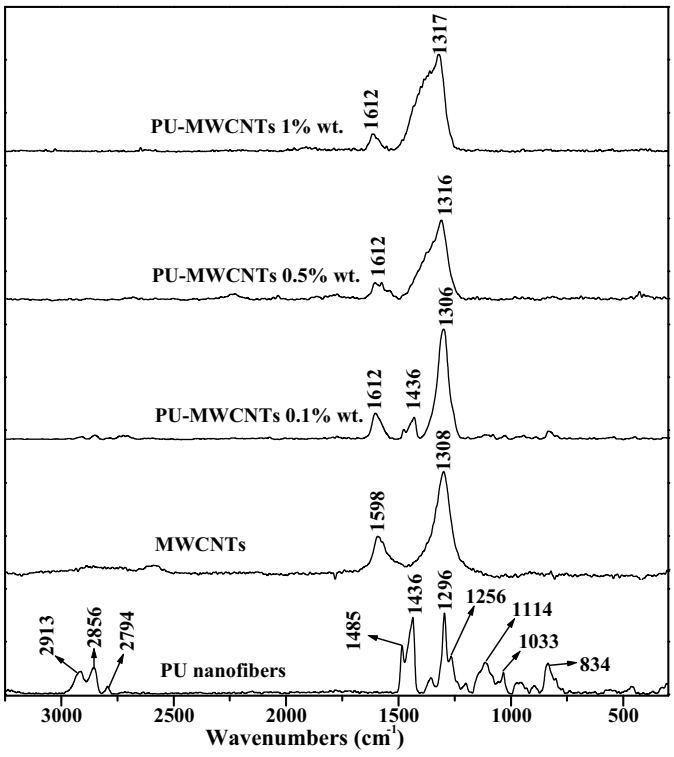

Fig. 6. Raman spectra of the polymer nanofiber, MWCNTs, and corresponding nanofibers containing MWCNTs.

the form of a "dog-bone" shape using a die that afforded samples with 2.75 mm wide at their narrowest point and a gauge length of 7.5 mm. At least five specimens were tested for tensile behavior and the average values were reported.

2.10. Cell imaging

Chemical fixation of cells on the nanofibers surfaces was carried out after 3 days of incubation. The procedure involved nanofiber samples being rinsed twice with phosphate buffer saline (PBS)

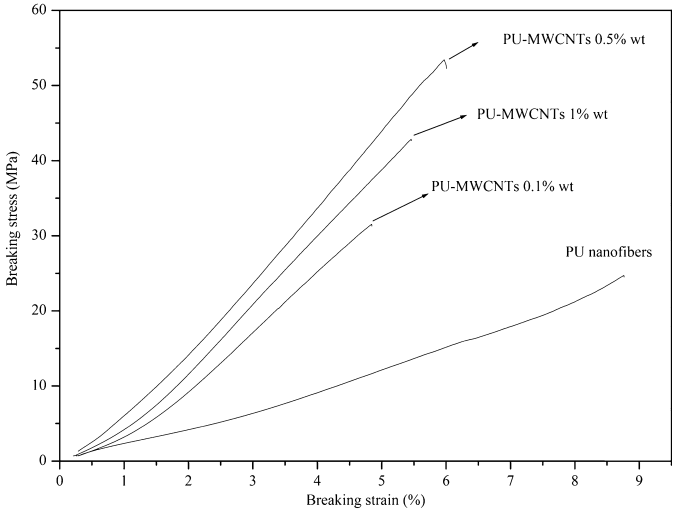

Fig. 7. Breaking stress vs. breaking strain curves for PU and PU-MWCNTs nanofibers.

Table 1
Mechanical properties of nanofibers.

Nanofiber	Young's modulus (MPa)	Breaking stress (MPa)	Breaking strain (mm/mm)	Maximum peak load (N)	Energy at maximum load (N-mm)
PU nanofiber	4.9 ± 1.2	26 ± 5	9.0 ± 0.1	1.6 ± 0.1	46 ± 2
PU-MWCNTs 0.1% wt.	8.3 ± 2.2	37 ± 6	5.6 ± 0.6	2.8 ± 0.3	52 ± 9
PU-MWCNTs 0.5% wt.	11 ± 40	56 ± 24	6.3 ± 0.3	2.3 ± 0.2	50 ± 4
PU-MWCNTs 1% wt.	9.7 ± 0.8	47 ± 8	5.9 ± 0.5	3.4 ± 0.7	67 ± 1

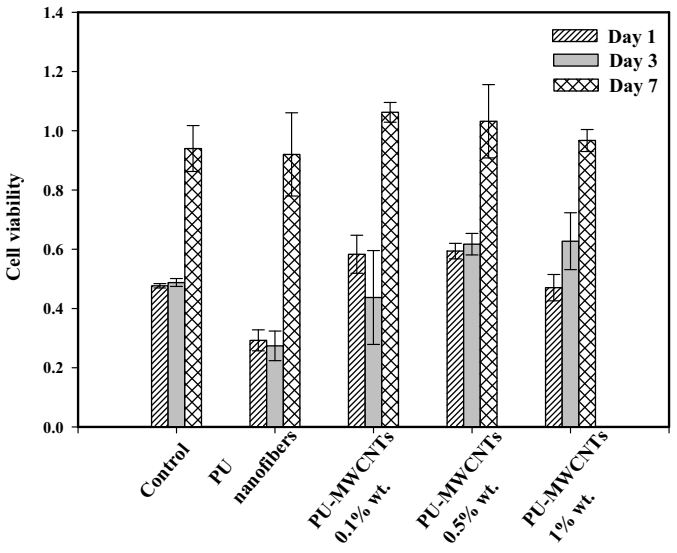

Fig. 8. Results from the MTT assay for NIH 3T3 fibroblasts in the presence of PU and PU-MWCNTs at 1, 3, and 7 days.

followed by fixation with a 2.5% vol. glutaraldehyde solution for 1 h. After cell fixation, the samples were rinsed with distilled water and then dehydrated with graded concentrations of ethanol (20, 30, 50, 70, and 100% vol. ethanol) for 10 min each [27]. Finally, the samples were kept overnight in a vacuum oven and observed in SEM to determine cell attachment. The samples for SEM were coated and observed under the same conditions as described previously.

3. Results and discussion

Scanning electron microscopy (SEM) was performed to confirm the formation of nanofibers (Fig. 1), which showed defect-free, bead-free morphologies. Fig. 1a and e present the electrospun PU fibers. The average fiber diameter for the PU nanofibers was 1000 ± 300 nm. Moreover, Fig. 1b and f shows micrographs for PU-MWCNTs 0.1% wt. with an average fiber diameter of 1000 ± 400 nm, while Fig. 1c and g are micrographs for PU-MWCNTs 0.5% wt. with an average fiber diameter of 700 ± 300 nm, and Fig. 1d and h present PU-MWCNTs 1% wt. resulting in an average fiber diameter of 600 ± 300 nm. Statistical analysis confirmed that the addition of 0.5% wt. and 1% wt. MWCNTs promoted a significant decrease ($p < 0.05$) in fiber diameter, but no difference in fiber diameter was observed between these groups (Fig. 2). Our research group has reported a similar decrease on nanofiber diameter upon addition of MWCNTs to electrospun polystyrene [28]. It is known that addition of MWCNTs decreases the resistivity of polymeric systems, which in turn promotes higher conductivity and higher charge density of the jet during electrospinning [29,30]. These effects result in the elongation of the fiber while it is being formed, promoting a decrease in fiber diameter, which is similar to reports where salts have been used as additives to reduce nanofiber diameter [31,32].

Transmission electron microscopy (TEM) was used to image the pristine MWCNTs (Fig. 3a and b), wherein their nanometer sized diameter and multiwalled structure is confirmed. Fig. 5 shows the PU-MWCNTs 1.0% wt. fibers, thus demonstrating the presence of the MWCNTs embedded within the polymer matrix. It is important to mention that it was not possible to image the electrospun fibers with lower concentrations of MWCNTs. The arrows marked in Fig. 4a and b evidence the presence of individual MWCNTs, confirming that the dispersion process was appropriate. Furthermore, these figures present the preferential alignment of MWCNTs along the fiber direction, but some of these MWCNTs tend to protrude from the fibers (Fig. 4c).

Fig. 5 shows the FTIR spectra for pure electrospun PU fibers and the corresponding fibers containing MWCNTs. Tecoflex® EG-80A is an aliphatic polyether-based thermoplastic polyurethane with peak assignments at 3500–3300 cm^{-1} for the free and bonded (respectively) hydrogen from the urethane bond (N–H) to the C=O. The peaks at 2942 and 2858 cm^{-1} are attributed to aliphatic symmetric and antisymmetric CH_2 stretching. Furthermore, the peak at 1720 cm^{-1} is for the C=O stretching from the amide I band, while the amide II band appears at 1530 cm^{-1} for N–H bending and C–N stretching, and the band at 1371 cm^{-1} corresponds to the CH_2 wagging. The C–N stretching at 1229 cm^{-1} is also known as the amide III band, while the aliphatic asymmetric C–O–C stretching is present at 1111 cm^{-1} [33–35]. The intermolecular interactions between the polymer and the MWCNTs were investigated by FTIR analysis, which showed minor changes in the spectra of the pure polymer nanofiber upon addition of MWCNTs. One of these subtle modifications was observed at the 3500–3300 cm^{-1} region, indicating that the π electrons present in MWCNTs interact with the hydrogen (free and bonded) attached to the nitrogen in the urethane bond, thus changing the shape of the band. The other change in the spectra was detected in the C–N stretching at 1229 cm^{-1}, with an increase in the wavenumber of the band to 1232 cm^{-1}, suggesting a non-specific non-covalent interaction between the σ bond in C–N and the π electrons from MWCNTs. Moreover, the vibrations caused in pristine MWCNTs indicate characteristic peaks at 1119, 1228, and 1437 cm^{-1} which is attributed due to the C=O groups in carbon nanotubes, used in this study.

Raman spectra of the PU fibers, MWCNTs, and the electrospun fibers containing MWCNTs are presented in Fig. 6. The peaks in the PU fibers spectrum situated at 2913, 2856, and 2794 cm^{-1} correspond to the aliphatic CH_2 stretching, while the peaks at 1485 and 1436 cm^{-1} are due to the aliphatic CH_2 bending. The 1296 cm^{-1} and its shoulder at 1256 cm^{-1} peaks are attributed to the C–O and C–N stretching, CNH bending, and the amide III. The aliphatic asymmetric C–O–C stretching from the ether groups appear at 1114 and 1033 cm^{-1}, and the peak at 834 cm^{-1} is assigned to the stretching, wagging, and twisting of the C–C and CH_2 in the polyether region of the polymer backbone [36,37]. The Raman spectrum of pristine MWCNTs shows the two vibrational modes expected, the tangential G-band at 1598 cm^{-1} and the D-band at 1308 cm^{-1} [38]. The additional spectra for PU-MWCNTs at different concentrations do not show the polymer peaks because these are "masked" by the presence of the MWCNTs. Nevertheless, the MWCNTs

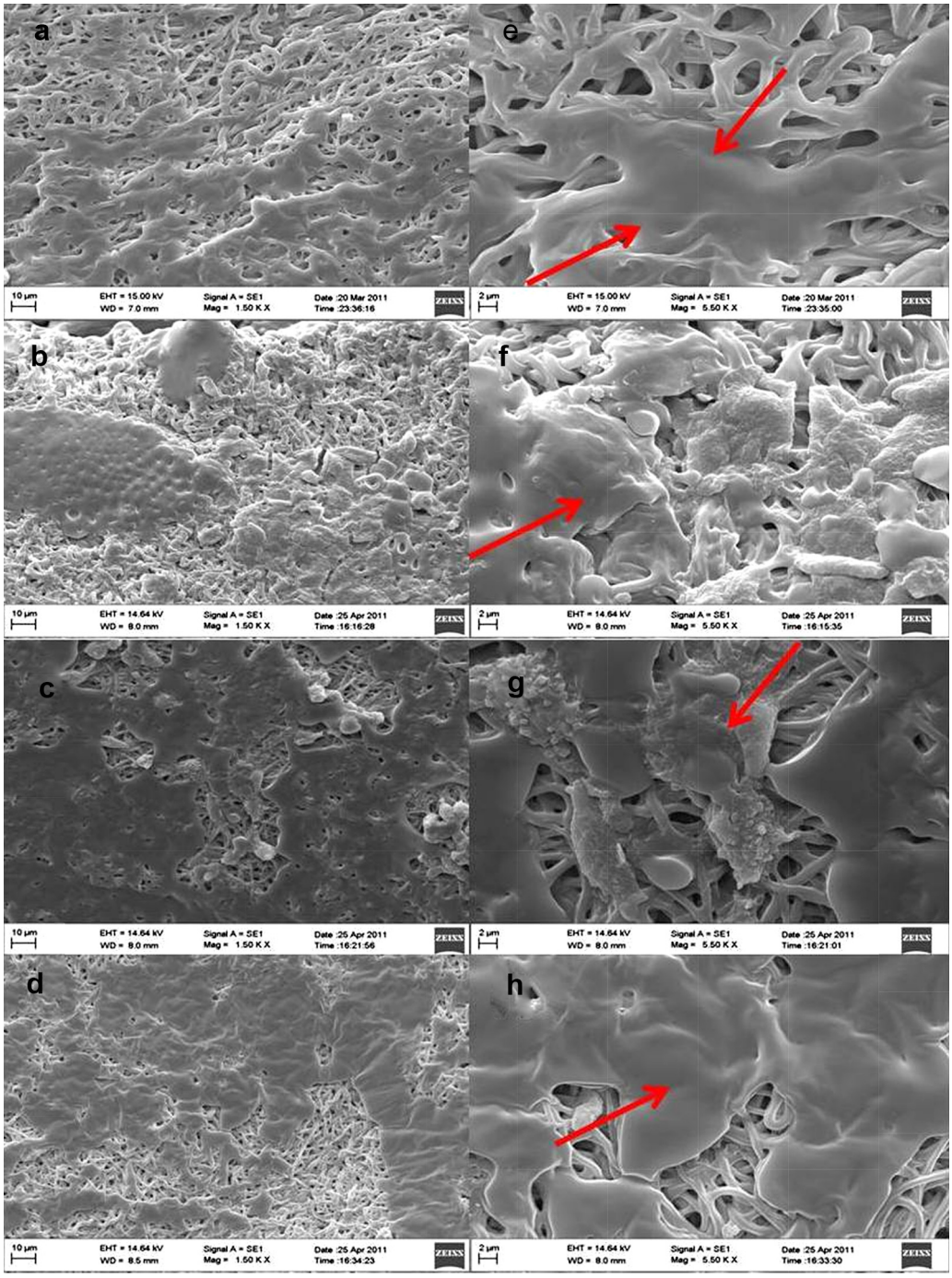

Fig. 9. Analysis of cell attachment by SEM after 3 days of fibroblasts culture. Nanofibers containing different amounts of MCNTs, (a) 0% wt., (b) 0.1% wt., (c) 0.5% wt., and (d) 1% wt. at 1.5 K magnification. Corresponding figures containing, (e) 0% wt., (f) 0.1% wt., (g) 0.5% wt., and (h) 1% wt. at 5.5 K magnification. Arrows indicate the appearance of cell patterns at specific location.

D- and G-bands broaden up and shift significantly to higher frequencies (up to 9 cm^{-1} for the D-band and 14 cm^{-1} for the G-band), with the notable exception of the D-band at PU-MWCNTs 0.1% wt. that showed a slight decrease. The shift to higher frequencies has been reported in the literature, indicating that the MWCNTs have debundled and polymer molecules are coating the surface of these materials and exerting pressure, thus the MWCNTs require more energy to vibrate and consequently higher wavenumbers [36]. Hence, Raman spectroscopy confirms the effectiveness of the dispersion process in debundling the MWCNTs, as observed in the TEM micrographs. Furthermore, Raman confirms the intermolecular interactions observed in FTIR between the polymer fiber and the MWCNTs.

Fig. 7 shows the breaking stress vs. breaking strain curves for the fibers investigated, whereas Table 1 presents the data obtained from these curves. It is observed that the PU electrospun fibers had the lowest Young's modulus and the highest strain of all the materials prepared. Table 1 demonstrates that the Young's modulus for the fibers significantly increased ($p < 0.05$) upon addition of MWCNTs regardless of the concentration. A similar trend for tensile

breaking stress, where it is observed and proven statistically that 0.5% wt. and 1% wt. loadings increased ($p < 0.05$) this property, with a maximum in breaking stress being reached at 0.5% wt. In contrast, fiber strain decreased with addition of the MWCNTs (Table 1), evidencing that the nanotubes interact with the polymeric matrix, and because of these additives stiffness, diminished elongations were achieved ($p < 0.05$). Results for maximum peak load of the fibers are presented in (Table 1), which demonstrates that 0.1% wt., 0.5% wt., and 1% wt. MWCNTs significantly increased ($p < 0.05$) the peak load. Furthermore, this property reached a maximum at the highest MWCNTs concentration. Table 1 shows data for the energy at maximum load, which was analyzed by a one-way ANOVA, revealed that 1% wt. MWCNTs was the only concentration to exert a significant effect ($p < 0.05$) on the polymer fiber.

Fig. 8 presents the cell viability for the blank and the different fibers prepared. The data presented in this graph was analyzed utilizing a two-way ANOVA. The results of this study indicate that there was a significant decrease ($p < 0.05$) in cell viability in the presence of pristine polyurethane fibers at days 1 and 3. However, the fibers containing MWCNTs showed the same cell viability as the control, with the notable exception that 0.5% wt. MWCNTs increased it on these days ($p < 0.05$). The rationale to have less cell growth with the nanofibers having (1% wt. MWCNTs, can be concluded from TEM results (i.e., Fig. 4c) examination which indicates little protruding out of nanotubes from nanofibers. We believe that this poking out of MWCNTs from the nanofibers can hinder the cell growth when higher concentration of MWCNTs is used to modify nanofibers. In addition, there was a significant increase ($p < 0.05$) in cell viability at day 7 for all PU-MWCNTs fibers, demonstrating the biocompatibility of the electrospun materials.

Furthermore, Fig. 9 shows SEM micrographs demonstrating cell growth and attachment to the fibers at 3 days of NIH 3T3 seeding. Moreover, the high magnification images provide information about the cell growth pattern, which suggests that the fibroblasts grow preferably along the fiber direction. Therefore, these results suggest the potential to use the PU fibers and PU-MWCNTs fibers in tissue engineering applications.

4. Conclusion

Electrospinning of a medical grade, commercially available polyurethane (Tecoflex® EG 80A) and its corresponding composite fibers containing MWCNTs was successful. SEM confirmed the formation of defect-free, bead-free fibers, which decreased in fiber diameter when 0.5% wt. and 1% wt. MWCNTs were added. TEM micrographs showed the presence of the MWCNTs in the composite fibers, with preferred MWCNTs alignment along the fiber direction. FTIR spectroscopy was utilized to investigate the intermolecular interactions between the PU and the MWCNTs, which indicated that the π electrons from the MWCNTs interact with the hydrogen attached to the nitrogen (N–H) and the σ bond in C–N in the urethane bond. Raman spectroscopy corroborated the results obtained from FTIR, showing that the MWCNTs were debundled and embedded within the PU fibers. Tensile testing demonstrated that the PU fibers had low Young's modulus and the highest tensile strain, while addition of MWCNTs promoted higher Young's modulus of the fibers at the expense of strain. Finally, the PU and PU-MWCNTs showed biocompatibility and cell proliferation on their surfaces along the fibers direction. Hence, the materials reported demonstrate enhanced Young's modulus and breaking stress and have been characterized extensively through imaging and spectroscopy and shown to be biocompatible, suggesting that these fibers could potentially be used in tissue engineering applications.

Acknowledgements

This work was financially supported by NIH-NIGMS-NIA grant # 1SC2AG036825-01, for which JM is gratefully acknowledged. The authors wish to acknowledge Mr. Joseph D. Ventura from Bayer Materials Science for providing the Multiwalled Carbon Nanotubes used in these studies and Raul Salazar from Lubrizol Advanced Materials for providing Tecoflex EG® 80A. Faheem A Sheikh and Hern Kim do acknowledge the support by National Research Foundation of Korea (NRF) – Grants funded by the Ministry of Science, ICT and Future Planning (2012K1A3A1A30055020) and the Ministry of Education (2009-0093816), Republic of Korea.

References

[1] J. Doshi, D.H. Reneker, Electrospinning process and applications of electrospun fibers, J. Electrostat. 35 (1995) 151–160.
[2] D.H. Reneker, A.L. Yarin, Electrospinning jets and polymer nanofibers, Polymer 49 (2008) 2387–2425.
[3] F.A. Sheikh, T. Cantu, J. Macossay, H. Kim, Fabrication of polyvinylidene (PVDF) nanofibers containing nickel nanoparticles as future energy server materials, Sci. Adv. Mater. 3 (2011) 216–222.
[4] S. Pelfrey, T. Cantu, M.R. Papantonakis, D.L. Simonson, R.A. McGill, J. Macossay, Microscopic and spectroscopic studies of thermally enhanced electrospun PMMA micro- and nanofibers, Polym. Chem. 1 (2010) 866–869.
[5] S. Sahoo, L.T. Ang, J.C. Goh, S.L. Toh, Growth factor delivery through electrospun nanofibers in scaffolds for tissue engineering applications, J. Biomed. Mater. Res. Part A 93A (2010) 1539–1550.
[6] I.A. Rodriguez, P.A. Madurantakam, J.M. McCool, S.A. Sell, H. Yang, P.C. Moon, G.L. Bowlin, Mineralization potential of electrospun PDO-hydroxyapatite-fibrinogen blended scaffolds, Int. J. Biomater. 2012 (2012) 1–12.
[7] S.A. Sell, M.J. McClure, C.E. Ayres, D.G. Simpson, G.L. Bowlin, Preliminary investigation of airgap electrospun silk-fibroin-based structures for ligament analogue engineering, J. Biomater. Sci. Polym. Ed. 22 (2011) 1253–1273.
[8] M.P. Francis, P.C. Sachs, P.A. Madurantakam, S.A. Sell, L.W. Elmore, G.L. Bowlin, S.E. Holt, Electrospinning adipose tissue-derived extracellular matrix for adipose stem cell culture, J. Biomed. Mater. Res. Part A 100A (2012) 1647–1927.
[9] J.W. Boretos, Past, present and future role of polyurethanes for surgical implants, Pure Appl. Chem. 52 (1980) 1851–1855.
[10] S. Gogolewski, Selected topics in biomedical polyurethanes. A review, Colloid Polym. Sci. 267 (1989) 757–785.
[11] P. Vermette, H.J. Griesser, G. Laroche, R. Guidoin, Biomedical applications of polyurethanes, Tiss. Eng. Intellig. Unit (2001) 221.
[12] J.H. Han, J.D. Taylor, D.S. Kim, Y.S. Kim, Y.T. Kim, G.S. Cha, H. Nam, Glucose biosensor with a hydrophilic polyurethane (HPU) blended with polyvinyl alcohol/vinyl butyral copolymer (PVAB) outer membrane, Sens. Actuators B 123 (2007) 384–390.
[13] N. Hains, V. Friscic, D. Gordos, Testing electrostatic properties of polyurethane coated textiles used for protective clothing, Int. J. Cloth. Sci. Technol. 15 (2003) 250–257.
[14] M.S. Khil, D.I. Cha, H.Y. Kim, I.S. Kim, N. Bhattarai, Electrospun nanofibrous polyurethane membrane as wound dressing, J. Biomed. Mater. Res. B: Appl. Biomater. 67 (2003) 675–679.
[15] S. Iijima, Helical microtubules of graphitic carbon, Nature 354 (1991) 56–58.
[16] J.P. Salvetat, J.M. Bonard, N.H. Thomson, A.J. Kulik, L. Forró, W. Benoit, L. Zuppiroli, Mechanical properties of carbon nanotubes, Appl. Phys. A 69 (1999) 255–260.
[17] J.P. Salvetat-Delmotte, A. Rubio, Mechanical properties of carbon nanotubes: a fiber digest for beginners, Carbon 40 (2002) 1729–1734.
[18] B.G. Demczyk, Y.M. Wang, J. Cumings, M. Hetman, W. Han, A. Zettl, R.O. Ritchie, Direct mechanical measurement of the tensile strength and elastic modulus of multiwalled carbon nanotubes, Mater. Sci. Eng. 334 (2002) 173–178.
[19] M. Meo, M. Rossi, Prediction of Young's modulus of single wall carbon nanotubes by molecular-mechanics based finite element modelling, Compos. Sci. Technol. 66 (2006) 1597–1605.
[20] J. Viola, B. Lal, O. Grad, The emergence of tissue engineering as a research field, in: VA ABT report, National Science Foundation, Arlington, 2009.
[21] S. Sharma, S. Mohanty, D. Gupta, M. Jassal, A.K. Agrawa, R. Tandon, Cellular response of limbal epithelial cells on electrospun poly-(-caprolactone nanofibrous scaffolds for ocular surface bioengineering: a preliminary in vitro study, Mol. Vis. 17 (2011) 2898–2910.
[22] Y. Wang, H. Shi, J. Qiao, Y. Tian, M. Wu, W. Zhang, Y. Lin, Z. Niu, Y. Huang, Electrospun tubular scaffold with circumferentially aligned nanofibers for regulating smooth muscle cell growth, ACS Appl. Mater. Interfaces 26 (2014) 2958–2962.
[23] L. Jia, M. P. Prabhakaran, X. Qin, S. Ramakrishna, Guiding the orientation of smooth muscle cells on random and aligned polyurethane/collagen nanofibers, J. Biomater. Appl., 0(0) 1-14, DOI: 10.1177/0885328214529002.
[24] X. Li, R. Cui, W. Liu, L. Sun, B. Yu, Y. Fan, Q. Feng, F. Cui, F. Watari, The use of nanoscaled fibers or tubes to improve biocompatibility and bioactivity of biomedical material, J. Nanomater. (2013) 16, Article ID 728130.

[25] Z.X. Meng, W. Zheng, L. Li, Y.F. Zheng, Fabrication and characterization of three-dimensional nanofiber membrance of PCL-MWCNTs by electrospinning, Mater. Sci. Eng. 30 (2010) 1014–1021.
[26] S. düzyer, S.K. koç, A. hockenberger, E. evke, Z. Kahveci, A. uğuz, Effects of different sterilization methods on polyester surfaces, Tekstil ve Konfeksiyon 23 (2013) 319–324.
[27] F.A. Sheikh, N.A.M. Barakat, M.A. Kanjwal, S.H. Jeon, H.S. Kang, H.Y. Kim, Self synthesize of silver nanoparticles in/on polyurethane nanofibers: nano-biotechnological approach, J. Appl. Polym. Sci. 115 (2010) 3189–3198.
[28] J. Macossay, A. Ybarra, F.A. Sheikh, T. Cantu, T.M. Eubanks, E. López-Cuéllar, N. Mohamed-Noriega, Electrospun polystyrene-multiwalled carbon nanotubes: imaging, thermal and spectroscopic characterization, Des. Monomers Polym. 15 (2012) 197–205.
[29] Y. Dror, W. Salalha, R.L. Khalfin, Y. Cohen, A.L. Yarin, E. Zussman, Carbon nanotubes embedded in oriented polymer nanofibers by electrospinning, Langmuir 19 (2003) 7012–7020.
[30] E.J. Ra, K.H. An, K.K. Kim, S.Y. Jeong, Y.H. Lee, Anisotropic electrical conductivity of MWCNT/PAN nanofiber paper, Chem. Phys. Lett. 413 (2005) 188–193.
[31] N.A.M. Barakat, M.A. Kanjwal, F.A. Sheikh, H.Y. Kim, Spider-net within the N6, PVA and PU electrospun nanofiber mats using salt addition: novel strategy in the electrospinning process, Polymer 50 (2009) 4389–4396.
[32] H. Fong, I. Chun, D.H. Reneker, Beaded nanofibers formed during electrospinning, Polymer 40 (1999) 4585–4592.
[33] S.J. McCarthy, G.F. Meijs, N. Mitchell, P.A. Gunatillake, G. Heath, A. Brandwood, K. Schindhelm, In- vivo degradation of polyurethanes: transmission-FTIR microscopic characterization of polyurethanes sectioned by cryomicrotomy, Biomaterials 18 (1997) 1387–1409.
[34] C. Guignot, N. Betz, B. Legendre, A.L. Moel, N. Yagoubi, Influence of filming process on macromolecular structure and organization of a medical segmented polyurethane, J. Appl. Polym. Sci. 85 (2002) 1970–1979.
[35] C. Zhang, Z. Ren, Z. Yin, H. Qian, D. Ma, Amide II and amide III bands in polyurethane model soft and hard segments, Polym. Bull. 60 (2008) 97–101.
[36] L.I. Maklakov, V.L. Furer, V.V. Alekseev, A.L. Furer, Investigation of the vibrational spectra of 2,6- and 4,6-polyurethanes and hexamethylenedimethylurethane, J. Appl. Spectrosc. 31 (1979) 1285–1289.
[37] V. Romanova, V. Begishev, V. Karmanov, A. Kondyurin, M.F. Maitz, Fourier transform Raman and Fourier transform infrared spectra of cross-linked polyurethaneurea films synthesized from solutions, J. Raman Spectrosc. 33 (2002) 769–777.
[38] A. Liu, I. Honma, M. Ichihara, H. Zhou, Poly(acrylic acid)-wrapped multiwalled carbon nanotubes composite solubilization in water: definitive spectroscopic properties, Nanotechnology 17 (2006) 2845–2849.